Resonance states in the ^{12}C-^{12}C Morse potential

Kiyoshi Katō
Department of Physics, Hokkaido University, Sapporo 060, Japan

Yasuhisa Abe
Yukawa Institute for Theoretical Physics, Kyoto University, Kyoto 606, Japan

(Received 23 October 1995; revised manuscript received 29 July 1996)

We investigate resonance states of the Morse plus centrifugal potential which has been used to explain the observed $^{12}C+^{12}C$ resonances by Satpathy *et al.* It is found that most of the enhancements in their calculated cross sections do not correspond to real resonances, but to so-called echoes. Furthermore, resonance poles of the Morse potential are searched exhaustively by the use of the complex scaling method. There are no resonance poles found in the higher energy region where many resonances are observed experimentally. We therefore conclude that the Morse potential is not appropriate for a comprehensive explanation of a series of resonances in the $^{12}C+^{12}C$ system. [S0556-2813(97)01704-4]

PACS number(s): 21.60.Gx, 25.70.Ef

I. INTRODUCTION

Since the discovery [1] of the resonances in the $^{12}C+^{12}C$ system near the Coulomb barrier, many resonances have been observed in various combinations of lighter heavy ions in incident as well as in outgoing channels, as accelerators and detector systems are developed. At energies well above the Coulomb barrier, resonances were observed systematically in inelastic channels with the excitations of the low-lying collective states 2^+, 3^-, ... of the incident ions, which were successfully explained by the band crossing model (BCM) [2]. Recently a new resonance has been observed by Wuosmaa *et al.* [3] in the inelastic channel of the $^{12}C+^{12}C$ system with both ^{12}C excited to the famous 0_2^+ state. The new resonance state is naturally expected to have a certain structure consisting of 6α clusters, since the 0_2^+ state is known to have the 3α structure.

As an interesting possibility, a linear chain configuration of six α particles was discussed [4]. On the other hand, based on the success of the BCM in the collective excitations, another interpretation was proposed: The resonance has the 6α-cluster configuration of weakly coupled two $^{12}C(0_2^+)$ [5]. A simple band crossing diagram calculated with the diagonal folding potentials naturally explains the new resonance and predicts resonances in the inelastic channels with a single excitation of $^{12}C(0_2^+)$ and with mutual excitations of $^{12}C(0_2^+)$ and $^{12}C(3^-)$, respectively. Coupled-channel calculations [6] based on the BCM turned out to bring about such resonances in the respective outgoing channels. Furthermore, the calculated results are found to be consistent with the resonance observed in the $^{12}C_{gr}+^{12}C(0_2^+)$ channel which has been long known, but not yet understood well [27]. It should be noticed here that there are many other resonances observed in the $^{12}C+^{12}C$ system, most of which are not yet understood. Some of them are known to have large decay widths in ^{8}Be channels, etc., not in the inelastic channels [7]. Therefore, resonances in heavy-ion reactions are considered to be a manifestation of various nuclear configurations with relatively simple structures which have large overlaps with several outgoing channels.

Nevertheless, many efforts have been made to explain all the observed resonances by the single-channel description, i.e., as potential resonances. Of course, if it can reproduce the energy spectrum of all the observed resonances, it would be interesting, although the problem still remains how to explain the variety of decay properties in terms of only the radial degree of freedom for each orbital angular momentum.

Satpathy *et al.* [8–11] employed the long-ranged Morse potential between two carbon nuclei in order to obtain many vibrational states which are compared with observed resonance levels. They solve the following Schrödinger equation analytically by the use of Flügge approximation [12]:

$$\left[-\frac{\hbar^2}{2\mu}\frac{d^2}{dr^2}+V_M(r)+\frac{\hbar^2}{2\mu r^2}L(L+1)\right]\chi_{nL}(r) = E(n,L)\chi_{nL}(r), \tag{1}$$

where μ is the reduced mass of the system and $V_M(r)$ denotes the Morse potential which is supposed to stand for nuclear and Coulomb interactions,

$$V_M(r)=A+B(e^{-2\beta x}-2e^{-\beta x}), \tag{2}$$

$$x=(r-r_0)/r_0. \tag{3}$$

The obtained energy spectrum is

$$E(n,L)=A-B+\frac{\hbar^2}{2\mu r_0^2}\left\{2\beta\gamma(n+\tfrac{1}{2})-\beta^2(n+\tfrac{1}{2})^2 + L(L+1)-\frac{9(\beta-1)^2}{4\beta^4\gamma^2}L^2(L+1)^2 - \frac{3(\beta-1)}{\beta\gamma}(n+\tfrac{1}{2})L(L+1)\right\}, \tag{4}$$

where $\gamma=\sqrt{B/(\hbar^2/2\mu r_0^2)}$, and L and n are the relative angular momenta and vibration quanta, respectively. This expres-

 © 1997 The American Physical Society

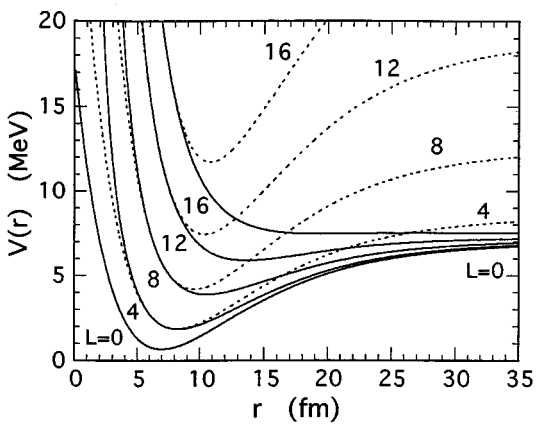

FIG. 1. The Morse-plus-centrifugal potentials (solid lines) and their Flügge approximated potentials (dotted lines) for $L=0$, 4, 8, 12, and 16.

sion of the energy spectrum has a similar form to the rotation-vibration spectrum [13] discussed by Erb and Bromley [14] and by Cindro and Greiner [15], though Satpathy *et al.* [8] consider it to be more general. Thus, they claim that the Morse potential model gives a concrete basis of the rotation-vibration approach. By fitting the experimental resonance spectrum, they determined the values of the parameters: $A=6.99$ MeV, $B=6.30$ MeV, $r_0=6.97$ fm, and $\beta=0.957$ [8]. However, for these parameter values, we should check the applicability of the Flügge approximation, by comparing original and approximated Morse plus centrifugal potentials. As shown in Fig. 1, the approximated reduced potentials (dashed lines) are not anything like the original reduced potentials (solid lines) in higher partial waves. And we can immediately understand that the original potentials do not sustain any bound state above about 7 MeV (barrier height), not only in lower partial waves, but also in higher ones. Therefore, as shown in Ref. [16], the energy spectrum given by Eq. (4) is false above 7 MeV, and comparisons with the experimental data above this energy are meaningless, though most of the resonances are observed there experimentally.

Of course, resonances could exist near barrier top energies, but not far above. So the above conclusion cannot be changed essentially, though there could be a few states around 7 MeV in addition to the correct bound states below. Satpathy and Sarangi [9], however, claimed that several resonances exist far above the barrier, corresponding to the bound states obtained previously with the inappropriate approximation. They, further, claimed that the potential has a resonance at $E_{\text{c.m.}}=32.5$ MeV for $L=14$ [11], which is considered to correspond to the new resonance observed by Wuosmaa *et al.*

So the purpose of the present paper is to precisely study resonances in the Morse potential they employed and to clarify whether the single-channel description still has the possibility to explain the observed resonances or not.

In Sec. II, we calculate the phase shifts and the cross sections which have enhancements similar to those of Satpathy *et al.* But it is found that almost all the ''resonances'' of Satpathy *et al.* are not true resonances, but echoes. In order to find out all the resonances exhaustively, we employ the complex scaling method. The resonance positions in the complex energy plane are determined for the Morse plus centrifugal potential in Sec. III. In Sec. IV, we discuss the resonance states of the modified Morse potential which has the Coulomb tail in the asymptotic distances. The final section, Sec. V, is devoted to a summary and conclusion.

II. PHASE SHIFTS OF THE MORSE POTENTIAL MODEL: RESONANCES AND ECHOES

In order to obtain correct resonance states of the Morse potential, we recalculate the phase shift $\delta_L(E_{\text{c.m.}})$ and the cross section $\sigma_L(E_{\text{c.m.}})$ in the same way as Refs. [9–11]. A channel radius a is introduced; in the outer region $r>a$, the asymptotic solution is given by

$$\chi^{\text{out}}_{L,k}(r)=kr[j_L(kr)-\tan\delta_L n_L(kr)], \tag{5}$$

where $j_L(kr)$ and $n_L(kr)$ are the spherical Bessel and Neumann functions with momentum $k=\sqrt{2\mu(E_{\text{c.m.}}-A)/\hbar^2}$. Here, it should be noted that the momentum k is measured from the barrier height A of the Morse potential. The solutions $\chi^{\text{in}}_{L,k}(r)$ in the inside region $r\leqslant a$ are calculated by numerical integration of the Schrödinger equation (1). The phase shift $\delta_L(E_{\text{c.m.}})$ is obtained from the continuity condition of logarithmic derivative at the channel radius a. Since the Morse potential used here has a very long range, we have to take $a\geqslant 80$ fm in order for the obtained phase shift $\delta_L(E_{\text{c.m.}})$ to be independent of the value of a as usual. With the phase shift, the partial cross section is calculated as

$$\sigma_L(E_{\text{c.m.}})=\frac{4\pi}{k^2}(2L+1)\sin^2\delta_L(E_{\text{c.m.}}), \tag{6}$$

where an additional factor of 2 is necessary in the right-hand side (RHS) due to the bosonic character of ^{12}C nuclei, but is neglected for the sake of comparison with Refs. [9–11].

The phase shifts and partial cross sections obtained for $L=8$ and 14 are presented in Fig. 2 as typical examples. As was shown in Ref. [16] and will be discussed later, the $L=8$ solutions of the Morse potential have five bound states. Then the phase shift $\delta_8(E_{\text{c.m.}})$ has to start from 5π at $E_{\text{c.m.}}=$A, according to the Levinson theorem. The calculated phase shift $\delta_8(E_{\text{c.m.}})$ shows a resonance behavior at very low energies $[(E_{\text{c.m.}}-A)<0.2$ MeV]. The detailed behavior of $\delta_8(E_{\text{c.m.}})$ in the region of $(E_{\text{c.m.}}-A)<0.2$ MeV is presented in Fig. 3. We find a very sharp resonance at $E_{\text{c.m.}}-A=0.036$ MeV with a width $\Gamma\sim 10^{-5}$ MeV. This resonance has been looked over by Satpathy *et al.* [9,10], perhaps due to its extreme sharpness. One may overlook such a sharp resonance if one looks only at the phase shift. With the aid of the results of the complex scaling calculation discussed later, we can find a resonance behavior in the phase shifts with very small energy meshes around the resonance region.

Above the sharp resonance energy, the phase shift $\delta_8(E_{\text{c.m.}})$ increases until $(E_{\text{c.m.}}-A)\sim 0.14$ MeV. This increasing of $\delta_8(E_{\text{c.m.}})$ is also due to the existence of real resonance states. However, the phase shift no longer increases by $\pi/2$. Therefore, it is difficult to determine the resonance energy E_r with the condition of $\delta_L(E_r)=\pi/2$ (modulo π). In such cases, it may be possible to determine

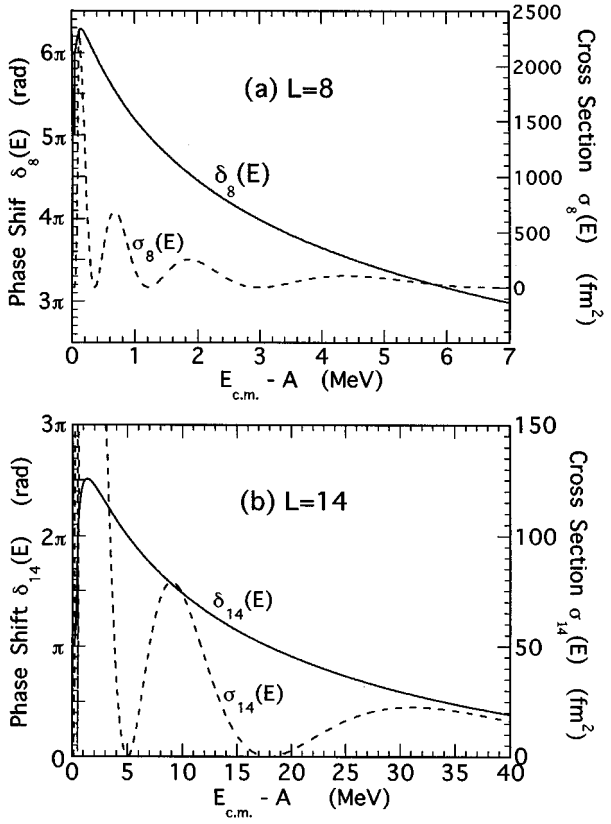

FIG. 2. Phase shifts (solid lines) and cross sections (dotted lines) of (a) $L=8$ and (b) $L=14$ states calculated with the Morse-plus-centrifugal potential.

the resonance energy from a crossing point of the calculated phase shift with a hard-sphere-scattering phase shift which is frequently displaced by $n\pi$ due to the existence of bound or resonance states at lower energies. To calculate the hard-sphere-scattering phase shift, we must introduce a hard-sphere-radius parameter a_h. For the usual short-range potentials between nuclei, a_h is taken to be a little larger than the sum of nuclear radii. However, in the present case of the very-long-range potential in comparison with 2 times the carbon radius, it is not easy to know how to choose the hard-sphere radius a_h. In addition, this method cannot be

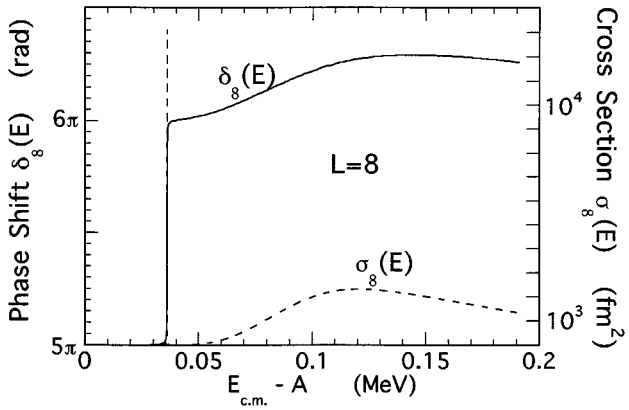

FIG. 3. Resonance behavior in phase shift (solid line) and cross section (dotted line) of $L=8$ in the very low energy region.

applied to overlapping resonances where resonance widths are larger than the distance between neighboring resonances. Actually the present Morse potential has two overlapping resonances in the energy region of $(E_{\text{c.m.}}-A)=0.06$–0.08 MeV as will be shown later.

In the energy region that $(E_{\text{c.m.}}-A)$ is larger than 0.14 MeV, the phase shift $\delta_8(E_{\text{c.m.}})$ only decreases. The monotonously decreasing $\delta_8(E_{\text{c.m.}})$ crosses $\pi/2$ (modulo π) at several energies with negative slopes, i.e., negative derivatives with respect to energy. It is well known that the resonance should have an increasing phase shift with energy [17]. From this definition of resonances, we conclude that there is no resonance in energies $(E_{\text{c.m.}}-A)>0.14$ MeV. However, the cross section shows an enhancement at energies where the phase shift crosses $\pi/2$ (modulo π), even if the energy derivative is negative. Such an enhancement of the cross section is associated with a flux advanced rather than delayed [17]; i.e., one has a negative width if one sticks to the resonance description. They are not true resonances but ''echoes'' [18].

In order to show the difference in the physical characters of resonance and echo, we present the wave functions corresponding to the resonances and the echoes in Fig. 4. The resonance wave functions are drastically changed by the potential from a free wave function. For example, a wave function has $(n+1)$ nodal points in the potential range, where n is numbers of bound or resonance states existing below the energy of the resonance under consideration. On the other hand, the wave function of the ''echo'' has almost no change even in the potential region. Therefore, we can say that the wave function of the ''echo'' is almost the same as a free wave function only except for a shift of the phase at an asymptotic distance, like real echoes which are reflected back with a time delay or phase shift [18]. Since the wave function of an echo is not concentrated in the interaction range, no enhancements are expected in other reaction channels even if they couple to the incident channel at the echo. Therefore, echoes should not be compared with any enhancements observed in reaction channels.

Although the phase shift presented in Fig. 30 of Ref. [10] shows a sharp increase like a step function at energies where the cross section has peaks, it seems to be due to an artificial jump by π in the computer calculation of $\tan^{-1}(x)$ whose range is $-\pi/2<\tan^{-1}(x)<\pi/2$. Therefore, we have to connect it smoothly by displacing by π. If there were true resonances, such jumps should become dull in higher-lying resonances from a physical point of view; the derivative $d\delta_L/dE_{\text{c.m.}}$, which is proportional to the decaying width, becomes larger as the energy increases, because the decaying width (lifetime) of higher energy potential resonances becomes larger (shorter).

As was mentioned above, the elastic cross section has enhancements also at energies of ''echoes.'' Satpathy *et al.* [9–11] called all the enhancements of the cross section ''resonances.'' But most of the peaks in the cross sections do not correspond to real resonances. The reason why many echoes appear with rather strong enhancements in the cross section at low energies can be explained by the long-range character of the present Morse potential. Usually, in nuclear physics, such enhancements due to echoes do not appear in the low energy region. Phase shifts very gradually decrease

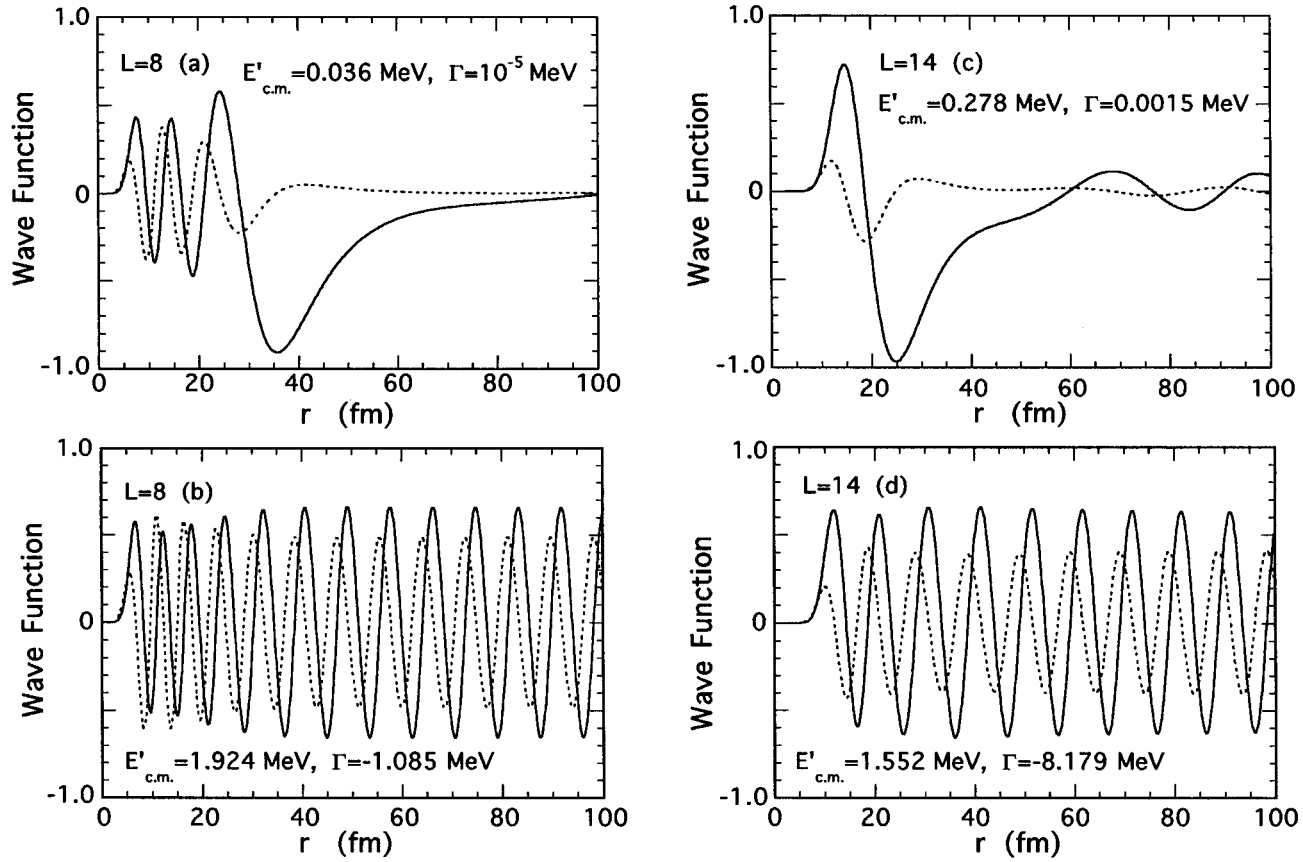

FIG. 4. Resonance and echo wave functions. Solid and dotted lines represent real and imaginary parts, respectively. For $L=8$, (a) resonance and (b) echo. For $L=14$, (c) resonance and (d) echo. Energies $E'_{\text{c.m.}}$ are measured from the asymptotic barrier constant A; i.e., $E'_{\text{c.m.}}=E_{\text{c.m.}}-A$.

after the resonance energy region, since the hard-sphere radius is not so large. Therefore, even if echoes appear, the ''widths'' ($\Gamma\propto 1/|d\delta/dE_{\text{c.m.}}|$) become very large. And then enhancements of the cross section are usually very small.

Although we have discussed only the result of $\delta_8(E_{\text{c.m.}})$, the behaviors are similar in the other partial waves. Satpathy and Sarangi [11] have discussed the new resonance ($L=14$) observed by Wuosmaa *et al.* [3] with the Morse potential. However, the peaks of the cross section assigned to the observed resonances are found to be also due to the ''echoes.'' They are not resonances.

III. COMPLEX SCALING METHOD FOR THE MORSE POTENTIAL

In order to determine unambiguously and exhaustively the resonance positions of the Morse potential, we employ a direct method, the so-called complex scaling method [19,20]. The complex scaling $U(\theta)$ for the relative coordinate r is defined as

$$U(\theta)r\rightarrow re^{i\theta}, \tag{7}$$

where θ is a scaling parameter with real values of $0\leqslant\theta\leqslant\theta_{\max}$. For the Morse potential, $\theta_{\max}$ is $\pi/2$ because of the analyticity condition of the scaled potential. This complex scaling transforms the Schrödinger equation (1) into the form

$$\left[-e^{-2i\theta}\frac{\hbar^2}{2\mu}\frac{d^2}{dr^2}+V_M(re^{i\theta})+e^{-2i\theta}\frac{\hbar^2}{2\mu r^2}L(L+1)\right]\chi_L^\theta(r)$$
$$=E^\theta(L)\chi_L^\theta(r). \tag{8}$$

According to the Aguilar-Balslev-Combes (ABC) theorem [19], the energies (negative real values) of bound states are independent of θ, and resonance energies (E_r) and widths (Γ) of the resonance solutions are obtained as real and imaginary parts of complex energies $E^\theta(L)$, that is, $E^\theta(L)=E_r-i\Gamma/2$, independently of θ for $\theta>\frac{1}{2}\tan^{-1}(\Gamma/2E_r)$. The complex scaled resonance wave functions $\chi^\theta_{r,L}(r)$ have dumping asymptotic forms, though they diverge exponentially in the nonscaled case. Therefore, we can solve resonance states with a boundary condition of $\chi^\theta_{r,L}(r)\rightarrow 0$ $(r\rightarrow\infty)$ in the same way as bound states.

We numerically solve bound and resonance states by using the renormalized Numerov method, which has been developed by Johnson [21] to calculate eigenvalues of bound states with numerically high accuracy. We here briefly explain the method with an extension to resonance eigenvalues in the complex scaling method.

The renormalized Numerov method is a general method to solve the second order differential equation

$$\left[\frac{d^2}{dr^2}+Q_L(r)\right]\chi(r)=0, \tag{9}$$

by using the three-term recurrence relation [22]

$$(1-T_{i+1})\chi_{i+1}-(2+10T_i)\chi_i+(1-T_{i-1})\chi_{i-1}=0, \tag{10}$$

where

$$\chi_i=\chi(r_i) \quad \text{and} \quad T_i=-\frac{h^2}{12}Q_L(r_i). \tag{11}$$

Here h is a spacing between grid points, and in the present case $Q_L(r_i)$ is given as

$$Q_L(r_i)=e^{2i\theta}\frac{2\mu}{\hbar^2}\left[E^\theta(L)-V_M(r_ie^{i\theta})-e^{-2i\theta}\frac{\hbar^2}{2\mu r_i^2}L(L+1)\right]. \tag{12}$$

Substituting $F_i=(1-T_i)\chi_i$ into Eq. (10), we have

$$F_{i+1}-U_iF_i+F_{i-1}=0, \tag{13}$$

$$U_i=(1-T_i)^{-1}(2+10T_i). \tag{14}$$

Furthermore, by defining the ratio

$$R_i=F_{i+1}/F_i, \tag{15}$$

we can express Eq. (13) in the two-term recurrence relation

$$R_i=U_i-R_{i-1}^{-1}. \tag{16}$$

This recurrence is easily solved with the initial value $R_0^{-1}=0$ because $\chi(r_1)\neq 0$ and $\chi(r_0=0)=0$ into the forward direction.

In the same way, Eq. (13) can be solved in the inward direction by replacing F_i by the ratio

$$\overline{R_i}=F_{i-1}/F_i. \tag{17}$$

The two-term recurrence relation for the inward direction is expressed as

$$\overline{R_i}=U_i-\overline{R_{i+1}^{-1}}. \tag{18}$$

This recurrence equation is also solved with the initial value $\overline{R_N^{-1}}=0$ [or more precisely with $\overline{R_N^{-1}}=\exp(ikhe^{i\theta})$] for the bound states and the complex scaled resonance states with $\theta>\theta_r$ [$\theta_r=(1/2)\tan^{-1}(\Gamma/2E_r)$].

We introduce a matching point r_M, to which we solve Eq. (16) in the forward direction and Eq. (18) in the inward direction. Using the two solutions R_M and $\overline{R_{M+1}}$ at the matching point r_M, we define

$$\overline{D}(E^\theta)=\overline{R_{M+1}^{-1}}-R_M \tag{19}$$

as a function of the energy. The equality $R_M=\overline{R_{M+1}^{-1}}$ [$\overline{D}(E^\theta)=0$] should be satisfied only if E^θ is an eigenvalue. This equality condition of the wave function χ_i may be replaced by the continuity condition of the logarithmic derivative of the wave function. From this condition, we have a function $D(E^\theta)$ [21], instead of $\overline{D}(E^\theta)$, which is defined as

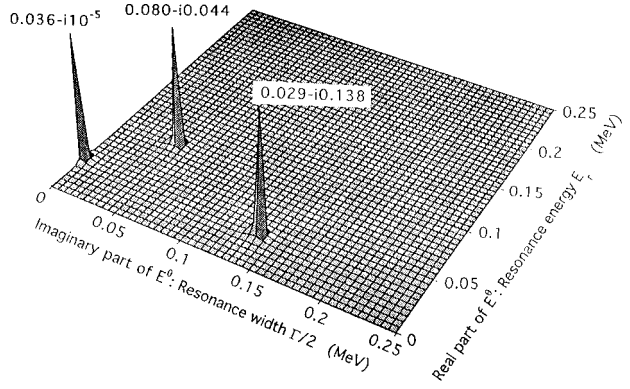

FIG. 5. The function $|D(E^\theta)|$ for $L=8$ resonance states calculated in the complex scaling method with $\theta=0.8$ rad.

$$D(E^\theta)=[A_{M+1}(\overline{R_{M+1}^{-1}}-R_M)-A_{M-1}(\overline{R_M}-R_{M-1}^{-1})]\times(1-T_M), \tag{20}$$

where

$$A_i=(\tfrac{1}{2}-T_i)(1-T_i)^{-1}. \tag{21}$$

Searching the zero points of $D(E^\theta)$ [or $\overline{D}(E^\theta)$] for complex values of E^θ, we can find the energies of bound states and resonance positions for an adequate scaling angle θ. For the bound state solutions, we have confirmed the previous results of Ref. [16]. In Fig. 5, we show $1/|D(E^\theta)|$ for the resonance solutions of the angular momentum $L=8$. This result has been obtained for $r_{\max}=140$ fm, $r_M=40$ fm, $h=0.01$ fm, and $\theta=0.8$ rad. The energy mesh $\Delta E=0.005$ MeV is employed for real and imaginary parts. Three sharp peaks are found in the fourth quadrant of the complex energy plane. The first resonance with the very small width corresponds to the sharp increase of π in the phase shift $\delta_8(E_{\text{c.m.}})$ at $(E_{\text{c.m.}}-A)=0.036$ MeV discussed in the previous section. The second and third peaks correspond to resonances newly found here. It is difficult to find them in phase shift calculation.

The resonance energies of the second and third resonances are very close and have large decay widths. They therefore are called overlapping resonances. On the other hand, it is very interesting that the third resonance has a

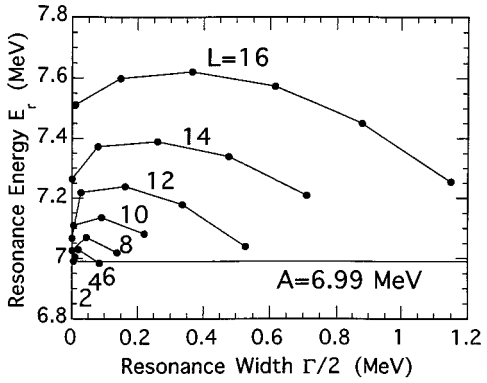

FIG. 6. Resonance positions, resonance energy (E_r) vs width ($\Gamma/2$), of the Morse-plus-centrifugal potential for $L=0-16$.

TABLE I. The bound state energies (above the dotted line) and resonance energies with widths (in parentheses) of the Morse-plus-centrifugal potential for the $^{12}C+^{12}C$ system.

$L \backslash n$	0	1	2	3	4	5	6	7	8	9
0	1.314	2.465	3.486	4.377	5.137	5.767	6.267	6.636	6.875	6.983
2	1.713	2.852	3.853	4.714	5.437	6.021	6.478	6.778	6.953	6.992 (0.011)
4	2.468	3.548	4.477	5.260	5.896	6.388	6.738	6.946	7.005 (0.019)	6.949 (0.328)
6	3.390	4.377	5.188	5.857	6.377	6.748	6.970	7.029 (0.039)	6.985 (0.168)	
8	4.361	5.207	5.895	6.428	6.807	7.026 (10^{-5})	7.070 (0.087)	7.019 (0.276)	6.900 (0.400)	
10	5.308	6.004	6.540	6.914	7.110 (0.010)	7.136 (0.181)	7.082 (0.442)	6.934 (0.730)		
12	6.182	6.710	7.040	7.067 (10^{-6})	7.220 (0.055)	7.240 (0.324)	7.180 (0.672)			
14	6.941	7.265 (0.001)	7.390 (0.522)	7.340 (0.954)	7.210 (1.42)					
16	7.512 (0.021)	7.622 (0.730)	7.573 (1.230)	7.255 (2.30)						

larger decay width, but lower resonance energy, than the second one. This result indicates that there are no resonances at energies higher than the second resonance energy. Such a property of resonance states, the existence of the maximum resonance energies, has already been discussed by Rittby, Elander, and Brändas [23]. They called the upper limit of resonance energies the ''complex threshold'' $\epsilon^{L}_{\rm thre}$. It is reasonable that there exists a maximum energy for the potential resonances, because there is no way to keep the system for a long time inside the potential pocket at energies higher than the barrier top energy. As seen in Fig. 6, the existence of the maximum energies, i.e., of the complex thresholds, is also confirmed for other partial waves. For all the partial waves, values of the maximum energy are very small; for instance, in the $L=8$ case, $(\epsilon^{8}_{\rm thre}-A)=0.0796-i0.0437$ (MeV). The existence of a complex threshold at such low energies means that the Morse potential cannot explain most resonances of the $^{12}C+^{12}C$ system observed in higher energies.

One may ask whether there are resonance solutions with $L=8$ other than the above three resonances. But if they exist, they are to be found in the third quadrant of the second Riemann sheet for the complex energy, which corresponds to the wedge region below $\mathrm{Im}(k)=-\mathrm{Re}(k)$ line in the fourth quadrant of the complex momentum plane. They cannot be called physical resonances anymore, because they are too far from the real energy axis, and thereby their widths are too large to observe. In Table I, we summarize numerical results of resonance energies and widths obtained in the fourth quadrant ($\mathrm{Re}[E^{\theta}(L)]>A$ and $\mathrm{Im}[E^{\theta}(L)]\leqslant 0$) of the energy plane for $L=0-16$ with bound state energies. Because of the disappearance of a potential pocket in the Morse plus centrifugal potential at $L\simeq 16$, as seen from Fig. 1, the $L\geqslant 16$ solutions have only resonance, but no bound states. The $L=16$ resonance states start at $E_{\rm c.m.}=7.512$ MeV ($\Gamma=0.021$ MeV) and have the maximum resonance energy $\mathrm{Re}(\epsilon^{16}_{\rm thre})=7.622$ MeV. Similarly, the $L=18$ resonance states starting at $E_{\rm c.m.}=7.893$ MeV ($\Gamma=0.373$ MeV) have a ''complex threshold'' at $\epsilon^{18}_{\rm thre}=7.905-i0.443$ (MeV).

IV. MODIFIED MORSE POTENTIAL WITH THE COULOMB POTENTIAL TAIL

We have obtained the energy spectrum of the Morse potential which has asymptotically a constant tail A. For this potential, the solutions of energies below A are bound states, though their energies are positive because the energy is to be measured from the $^{12}C+^{12}C$ threshold. However, as was mentioned in Sec. II, the momentum k is defined by $\sqrt{2\mu(E_{\rm c.m.}-A)/\hbar^2}$ in the phase shift calculations. Such an artificial treatment of scattering states above A is due to the asymptotically unphysical form of the Morse potential.

In order to describe collisions between heavy ions, we have to use the Coulomb potential at asymptotic distances because of the finite range character of the nuclear potential. The Morse potential given in Eq. (2) should be interpreted to represent the sum of the nuclear and Coulomb interactions between nuclei. However, the Morse potential has a constant tail A which does not describe the correct Coulomb tail. It is very difficult to connect the Morse potential and the Coulomb potential smoothly, because the latter decreases more

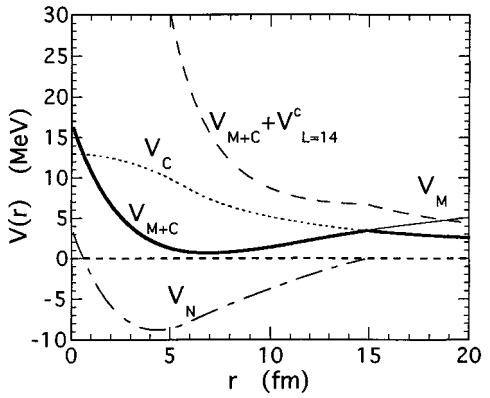

FIG. 7. The Coulomb potential (V_C, dotted line), the nuclear part (V_N, dash-dotted line) of the Morse potential (V_M, thin line), the modified Morse potential (V_{M+C}, thick line), and the modified Morse-plus-centrifugal ($L=14$) potential (dashed line).

than the constant tail A of the former at the asymptotic distance for connection.

Satpathy and Sarangi [9] tried to connect them by force by redefining the nuclear potential part of the Morse potential assuming the Coulomb potential

$$V_C(r)=\begin{cases} 1.438\dfrac{Z_P Z_T}{2R_c}\left(3-\dfrac{r^2}{R_c^2}\right), & r<R_c, \\ 1.438\dfrac{Z_P Z_T}{r}, & r>R_c, \end{cases} \tag{22}$$

where $R_c=1.3(A_P^{1/3}+A_T^{1/3})$ fm and $Z_P(Z_T)$ and $A_P(A_T)$ are the charge and mass numbers of a projectile (target) nuclei, respectively. In Fig. 7, we plot the Coulomb potential V_C, the nuclear potential part given by $V_N(r)=V_M(r)-V_C(r)$ with the Morse potential V_M. Here, we should notice that the positive part of V_N at $r>r_G$ is put to be zero, where r_G is defined by $V_M(r_G)=V_C(r_G)$. Then a modified potential having the Coulomb potential tail is defined by $V_{M+C}(r)=V_N(r)+V_C(r)$ [9,10]. The modified Morse potential $V_{M+C}(r)$ has a kinked barrier at $r=r_G$, whose height is lower than A of the Morse potential. In large distances, $V_{M+C}(r)$ has the Coulomb potential tail. Therefore, the modified Morse potential no longer has bound states with positive energies. Although a few low-lying bound states obtained with the Morse potential $V_M(r)$ may survive as resonance states, almost all bound states obtained previously with $V_M(r)$ disappear in the modified Morse potential $V_{M+C}(r)$.

In Fig. 8, we show the nuclear phase shift $\delta_L^N(E_{\rm c.m.})$ for $L=8$ and 14 calculated by subtracting the Coulomb part $\delta_L^C(E_{\rm c.m.})$ from the total phase shift $\delta_L(E_{\rm c.m.})$ for the modified Morse potential $V_{M+C}(r)$, where we should note that the energy is measured from the threshold, but not from the asymptotic potential height A. Since $V_{M+C}(r)\cong 0.69$ MeV at the potential minimum as seen in Fig. 7, the nuclear phase shift starts at $E_{\rm c.m.}\cong 0.69$ MeV. From the behavior of $\delta_{L=8}^N$, there exists a resonance at 4.34 MeV, which corresponds to the lowest bound state in the case of the Morse potential. The second bound state in the original Morse potential barely survives as a broad resonance at ~ 6 MeV. In $\delta_{L=14}^N$, we only obtain a broad resonance around 8 MeV. So the modified Morse potential gives a few resonances as the original one does. Furthermore, the calculated energies of a few resonances, measured from the threshold, are not in agreement with observed resonances. Again, many enhancements in the cross section calculated by Satpathy and Sarangi [9] come from echoes. Thus, we conclude that the potential V_{M+C} does not give an energy spectrum to be compared with the experiments.

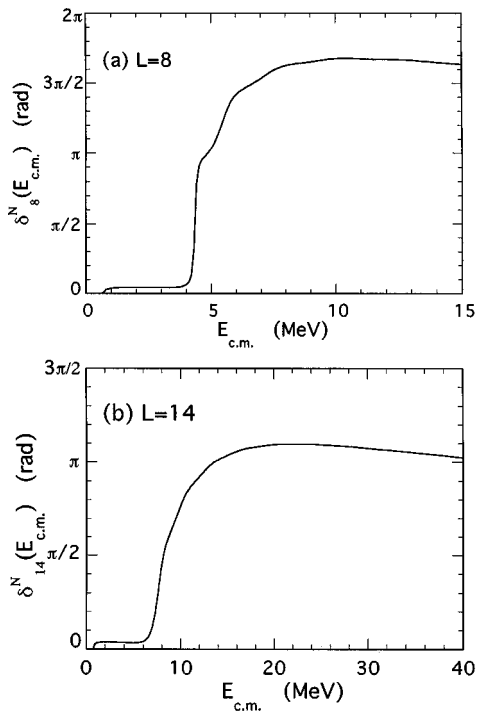

FIG. 8. Nuclear phase shifts δ_L^N (dotted lines) and total nuclear cross section σ_L (solid lines) of the modified Morse-plus-centrifugal potential V_{M+C} with the Coulomb potential tail for $L=8$ (a) and 14 (b).

On the other hand, Satpathy and Sarangi [9] claimed that the resonance energies estimated from the phase shifts calculated for the modified Morse potential $V_{M+C}(r)$ had a good correspondence with the bound state energies of the original one $V_M(r)$. However, it should be noticed that we have to use the momentum $k=\sqrt{2\mu E_{\rm c.m.}/\hbar^2}$ for the modified Morse potential, but not $k=\sqrt{2\mu(E_{\rm c.m.}-A)/\hbar^2}$ defined in the case of the original one. Furthermore, when the Coulomb potential works at an asymptotic distance, the resonance structure in the cross section has to be examined by subtracting the Coulomb cross section due to its divergent property. A direct comparison of the nuclear phase shift and cross section obtained from the modified Morse potential should not be made with those calculated for the original Morse potential which is supposed to stand for the nuclear plus the Coulomb potentials.

V. SUMMARY AND CONCLUSION

We have investigated the Morse potential model for the $^{12}C+^{12}C$ system as a typical example of the molecular resonances observed in many lighter heavy-ion collisions. Satpa-

thy *et al.* [9–11] have calculated phase shifts and cross sections with the Morse potential, and claimed that they obtained many resonances states in the energy region far above the barrier height of the Morse potential, which correspond to experiments. However, we have shown in this paper that most of ''resonances'' obtained by Satpathy *et al.* are not true resonances, but so-called echoes. Because of an unusually long-range form of the Morse potential, the phase shift rather sharply crosses several times $\pi/2$ (modulus) with negative derivative with respect to energy. Such a behavior of the phase shift is called an echo. Their wave functions are not trapped in the interaction region. Therefore they cannot show up themselves in any enhancements in reaction channels.

Careful searches for resonances by the use of the complex scaling method have shown that there are a few true resonances in extremely low energies, i.e., just above $E_{\text{c.m.}}=A=6.99$ MeV, and no resonances above ''the complex threshold;'' for instance, $\text{Re}(\epsilon^{L}_{\text{tore}})= A+0.0796$ MeV and $A+0.40$ MeV for $L=8$ and 14, respectively. Therefore, the Morse potential does not explain the resonances observed in $^{12}\text{C}+^{12}\text{C}$ systematically.

Satpathy and Sarangi [9] have proposed a Coulomb tail correction of the Morse potential so as to have the correct asymptotic behavior instead of the unphysical constant value A. And their conclusion was that several states survive as resonances and correspond to experiments. However, as shown above, there are only a few resonances near the barrier top and they have no correspondence, not only with those of the Morse potential, but also with experimental data, with a caution that the definition of energy has to be changed properly from the case of the Morse potential with a constant asymptotic value to the normal one. Particularly for the new resonance observed at $E_{\text{c.m.}}=32.5$ MeV, the obtained enhancement in Ref. [11] for $L=14$ partial waves is again due to an echo, but not due to a resonance.

Our conclusion on the Morse potential model is that it is not possible to explain most of the experimental resonance data of the $^{12}\text{C}+^{12}\text{C}$ system. Much experimental evidence in resonance phenomena observed through various reactions indicate that the importance of various configurations, especially those of the inelastic channels. However, it is impossible to describe such coupling properties within a single-channel potential model. It is rather natural to take into account the coupling with other degrees of freedom explicitly, which has been investigated by many authors. The BCM [2] is the most promising approach among them, and gives not only an intuitive understanding of the coupling mechanism, but also quantitative descriptions of many observed quantities. Recently, Hirabayashi *et al.* [6] have calculated the resonance cross section by using the BCM where many low-lying excited states including the 0^{+}_{2} state of the ^{12}C nucleus are taken into account. They successfully reproduced the experimental excitation function and the angular distributions of Wuosmaa *et al.* [3].

The Morse potential was first discussed in relation to the vibration-rotation model [13] only from the viewpoint of its energy spectrum. However, it is now clear that the Morse potential does not give the basis of the vibration-rotation model, because its energy level structure is shown to be completely different from that of the vibration-rotation model. In order to explain many ''vibrational'' levels with the same spin, the potential is forced to have an unphysically long-range form. But the long-range potential necessarily provides a strong rotation-vibration coupling as was discussed in a previous paper [16]. In the case of the strong rotation-vibration coupling, a simple rotation-vibration model breaks down in higher quantum states, even if the ratios $E_{\text{rot}}/E_{\text{vib}}$ [24] of the elementary energy quanta are very small. It is worth noticing that the ratio of the present case is the same order of magnitude as the collective excitations in ^{188}Os and ^{190}Os, but in the latter cases only states with small excitation quanta are discussed; so if those with higher quantum states are discussed, the rotation-vibration model would loose its validity as in the present case. Arguments based on a comparison with Os isotopes should be made carefully.

The Morse potential, thus, does not give a description of the ''rotation-vibration'' spectrum. A physical background of the empirical energy formula suggested by the vibration-rotation model might be realized by other approaches [25,26] if the empirical formula is physically meaningful. Cseh and co-workers [26] have recently developed an approach phenomenologically by taking into account many degrees of freedom of intrinsic excitations of ^{12}C in addition to the elastic $^{12}\text{C}+^{12}\text{C}$ channel.

The authors thank S. Aoyama for his help with numerical calculations of the complex scaling method.

[1] D. A. Bromley, J. A. Kuehner, and E. Almqvist, Phys. Rev. Lett. **4**, 365 (1960).
[2] Y. Abe, in *Nuclear Molecular Phenomena*, edited by N. Cindro (North-Holland, Amsterdam, 1978), p. 211; Y. Kondo, Y. Abe, and T. Matsuse, Phys. Rev. C **19**, 1356 (1979).
[3] A. H. Wuosmaa *et al.*, Phys. Rev. Lett. **68**, 1295 (1992).
[4] W. D. M. Rae, A. C. Merchant, and B. Buck, Phys. Rev. Lett. **69**, 3709 (1992).
[5] Y. Abe, Y. Kondo, and T. Matsuse, Prog. Theor. Phys. Suppl. **67**, 303 (1980).
[6] Y. Hirabayashi, Y. Sakuragi, and Y. Abe, Phys. Rev. Lett. **74**, 4141 (1995).
[7] R. M. Freeman, F. Haas, A. Elanique, A. Morsad, and C. Beck, Phys. Rev. C **51**, 3505 (1995).
[8] L. Satpathy, P. Sarangi, and A. Faessler, J. Phys. G **12**, 201 (1986).
[9] L. Satpathy and P. Sarangi, J. Phys. G **16**, 469 (1990).
[10] L. Satpathy, Prog. Part. Nucl. Phys. **29**, 327 (1992).
[11] L. Satpathy and P. Sarangi, J. Phys. G **20**, L37 (1994).
[12] S. Flügge, *Practical Quantum Mechanics* (Springer, Berlin, 1974), p. 182.
[13] F. Iachello, Phys. Rev. C **23**, 2778 (1981).
[14] K. A. Erb and D. A. Bromley, Phys. Rev. C **23**, 2781 (1981).
[15] N. Cindro and W. Greiner, J. Phys. G **9**, L175 (1983).

[16] K. Katō and Y. Abe, Prog. Theor. Phys. **80**, 119 (1988).
[17] R. G. Newton, *Scattering Theory of Waves and Particles* (Springer-Verlag, New York, 1966), p. 354.
[18] K. W. McVoy, Phys. Lett. **17**, 42 (1965).
[19] J. Aguilar and J. M. Combes, Commun. Math. Phys. **22**, 269 (1971); E. Balslev and J. M. Combes, *ibid.* **22**, 280 (1971).
[20] A. T. Kruppa and K. Katō, Prog. Theor. Phys. **84**, 1145 (1990).
[21] B. R. Johnson, J. Chem. Phys. **67**, 4086 (1977).
[22] S. E. Koonin, *Computational Physics* (Benjamin/Cummings, Menlo Park, 1986), p. 64.
[23] M. Rittby, N. Elander, and E. Brändas, Phys. Rev. A **24**, 1636 (1981).
[24] J. M. Eisenberg and W. Greiner, *Nuclear Models* (North-Holland, Amsterdam, 1970), Vol. 1, Chap. 6, Sec. 5.
[25] M. Ohkubo, K. Katō, and H. Tanaka, Prog. Theor. Phys. **67**, 207 (1982). Y. Suzuki and K. T. Hecht, Nucl. Phys. **A338**, 102 (1992).
[26] J. Cseh, G. Lévai, and W. Sheid, Phys. Rev. C **48**, 1724 (1993); J. Cseh and G. Lévai, Ann. Phys. (N.Y.) **230**, 165 (1994).
[27] S. F. Pate, R. W. Zurmühle, P. H. Kutt, and A. H. Wuosmaa, Phys. Rev. C **37**, 1953 (1988).